The Additive Nature of Energy Penalties in 10-Vertex *nido*-(Car)boranes

Farooq A. Kiani[a,b] and Matthias Hofmann*[a]

Keywords: Boranes / Carboranes / Density functional theory / Energy penalties / Structural increment system

A structural increment system, i.e. quantitative rules that govern the relative stabilities of 10-vertex *nido*-boranes and -carboranes, has been determined. Density functional theory computations at the B3LYP/6-311+G(d,p)//B3LYP/6-31G(d) level with ZPE corrections were carried out for 81 different boron hydride and carborane structures from $[B_{10}H_{12}]^{2-}$ to $C_3B_7H_{11}$ to determine their relative stabilities. A set of eleven disfavored geometrical features that destabilize a cluster structure relative to a hypothetical ideal situation were identified and weighted by so-called energy penalties. The latter show good additive behavior and allow us to reproduce the DFT computed relative energies mostly with an accuracy of 6.0 kcal mol^{-1}. Some unknown 10-vertex *nido*-carboranes that are thermodynamically more stable than their known isomers are also identified.

Introduction

Assuming a hypothetical, ideal cluster and additive destabilizations caused by deviating structural features, one can derive corresponding energy penalties that allow an easy estimation of the thermodynamic stabilities of cluster isomers. Such quantitative rules weighting different disfavored structural features of a particular heteroborane cluster have already been determined for 6-[1] and 11-vertex[2] *nido*-(car)boranes and 11-vertex *nido*-hetero(car)boranes.[3] These rules not only indicate the thermodynamically most stable isomer for a given formula,[2,3] but also describe the relative stabilities of different isomers quite accurately.[1–3] These systematic studies also identified some still unknown clusters of competitive thermodynamic stability which might be synthesized in the future.[2,3] Some structural features have similar energy penalties in 6- and 11-vertex *nido*-boranes, -carboranes, and even -heterocarboranes.

Here we extend the structural increment approach to the more complex 10-vertex *nido* cluster; 6- and 11-vertex *nido* clusters are quite simple as they have only one kind of cage (i.e., of the same connectivity, identified by k_c) and one kind of peripheral (k_p) vertex. A *nido* 6-vertex cluster has five $3k_p$ and one $5k_c$ vertices ($\Delta k = 2$), and an 11-vertex *nido* cluster has five $4k_p$ and six $5k_c$ vertices ($\Delta k = 1$). The situation is more complicated in the 10-vertex *nido* family, however, due to two different types of peripheral vertices, i.e. two $3k_p$ ($\Delta k = 2$) and four $4k_p$ ($\Delta k = 1$) next to the four $5k_c$ vertices (see Figure 1). These three different types of vertices make the 10-vertex *nido* cluster more complex and therefore some new and additional structural features need to be introduced. These features and their corresponding energy penalties have been derived and are discussed in this paper.

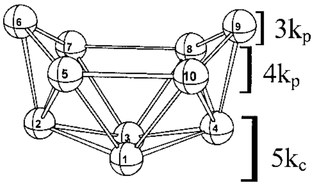

Figure 1. Cluster shape and numbering scheme for 10-vertex *nido*-boranes and -carboranes; 3*k*, 4*k*, and 5*k* indicate connectivities of peripheral (p) and cluster (c) vertices with respect to other cluster atoms.

Results and Discussion

Structural Features for 10-Vertex *nido*-Boranes and -Carboranes

Eleven energy increments corresponding to disfavoring structural features are sufficient to reproduce the relative stability order, as derived by DFT computations, for eighty-one 10-vertex *nido*-boranes and -carboranes ranging from $[B_{10}H_{12}]^{2-}$ to $C_3B_7H_{11}$. These energy penalties are listed in Table 1 and the corresponding structural features are illustrated in Figure 2.

The energy penalties can be divided into three main groups: *carbon structural features*, arising due to carbon-

---

[a] Anorganisch-Chemisches Institut, Ruprecht-Karls-Universität Heidelberg
Im Neuenheimer Feld 270, 69120 Heidelberg, Germany
Fax: +49-6221-544955
E-mail: matthias.hofmann@aci.uni-heidelberg.de
farooq.kiani@aci.uni-heidelberg.de
[b] Department of Chemistry, Quaid-I-Azam University, Islamabad 45320, Pakistan

Supporting information for this article is available on the WWW under http://www.eurjic.org or from the author.

DOI: 10.1002/ejic.200400982

Table 1. A comparison of energy penalties for 6-, 10- and 11-vertex *nido* clusters.

Increment name	Symbol	Energy penalties [kcal mol^{-1}]		
		6-vertex *nido*[a]	11-vertex *nido*[b]	10-vertex *nido*[c]
Carbon atom at 5*k* instead of 3*k*	$C_{3k\rightarrow5k}$	33	–	40.4
Carbon atom at 4*k* instead of 3*k*	$C_{3k\rightarrow4k}$	–	–	16.1
Carbon atom at 5*k* instead of 4*k*	$C_{4k\rightarrow5k}$	–	28.0	24.3[d]
endo-CH	CH_2	30	33.2	32.6
C(*endo*-CH)	$C(CH_2)$	10	(11.6)	–
C(*endo*-CH)C	$C(CH_2)C$	(17)	(20.4)	–
Bridge CH–B	CH–B	27	33.1	32.1
Bridge C–HB	C–HB	35	–	–
C(bridge-CH–B)	C(CH–B)	5	(7.3)	–
Adjacent carbon atoms.	CC	15	16.0	14.1
Adjacent carbon atoms (3*k*–5*k*)	CC(3–5)	–	–	3.3
endo-BH	BH_2	11	2.3	5.0
C(*endo*-BH)	$C(BH_2)$	7	(4.6)	–
C(*endo*-BH)C	$C(BH_2)C$	25	28.8	–
BHB(*endo*-H)BHB	H(*endo*-H)H	–	23.9	–
$(BHB)_2$(0–62)	HA_0	7	–	–
$(BHB)_2$	HH	–	25.9	2.9
C(BHB)	C(H)	–	2.2	–
5*k*C$(BHB)_2$(0–62)	5*k*(HA_0)	5	–	–
$(BHB)_2$(1–43)	HA_1	11	–	–
5*k*C$(BHB)_2$(1–43)	5*k*(HA_1)	(2)	–	–
BHB(c)BHB	H(C)H	–	–	8.7
BHB connected to 4*k* vertices	H(4–4)	–	–	12.7
3*k*(open-face BHB)	3*k*C(H)	–	–	13.7

[a] See ref.[1] [b] See ref.[2] [c] This work. [d] $C_{4k\rightarrow5k}$ is not an independent structural feature in the 10-vertex *nido* cluster, but results as the difference between $C_{3k\rightarrow4k}$ and $C_{3k\rightarrow5k}$.

atom positions, *hydrogen structural features*, arising due to hydrogen-atom placement, and *mixed structural features*, which involve both carbon and hydrogen atoms.

Carbon Structural Features

$C_{3k\rightarrow5k}$

A carbon atom at a 5*k* (vertices 1 through 4) rather than a 3*k* position (vertices 6 and 9) destabilizes a structure by 40.4 kcal mol^{-1}.

$C_{3k\rightarrow4k}$

A carbon atom has an energy penalty of 16.1 kcal mol^{-1} when it is at a 4*k* position (i.e. positions 5, 7, 8, or 10) rather than a 3*k* position.

CC and CC(3–5)

Two adjacent carbon atoms are unfavorable, but the amount of destabilization depends upon the carbon atoms' connectivities: for $\Delta k = 0$ and 1 the CC energy penalty is 14.1 kcal mol^{-1}, whereas for $\Delta k = 2$, (i.e., adjacent 3*k* and 5*k* C atoms), a considerably smaller CC(3–5) energy penalty of only 3.3 kcal mol^{-1} is found.

Hydrogen Structural Features

H(4–4)

A hydrogen atom bridging to two 4*k* vertices (rather than a 3*k* and a 4*k* boron vertex) results in an increased energy of the cluster by 12.7 kcal mol^{-1}.

BH_2

An *endo*-terminal hydrogen atom attached to a boron atom has an energy penalty of 5.0 kcal mol^{-1}.

HH

Adjacent hydrogen atoms are accompanied by an energy penalty of 2.9 kcal mol^{-1}.

Mixed Structural Features

CH_2

An *endo*-terminal hydrogen atom at a carbon atom results in an energy penalty of 32.6 kcal mol^{-1}. In all structures considered here, except **JR**, the CH_2 group is located at a 3*k* vertex.

CH–B

An *endo*-hydrogen atom bound to a carbon atom but bent towards a boron atom, i.e. bridging between a carbon atom and a boron atom, is disfavored by 32.1 kcal mol^{-1}.

3kC(H)

A 3*k* carbon atom in the presence of one or more bridging hydrogen atoms at the open face results in a 13.7 kcal mol^{-1} destabilization.

H(C)H

One or two carbon atoms entrapped between two hydrogen bridges through one connection only, incorporate a penalty of 8.7 kcal mol^{-1}.

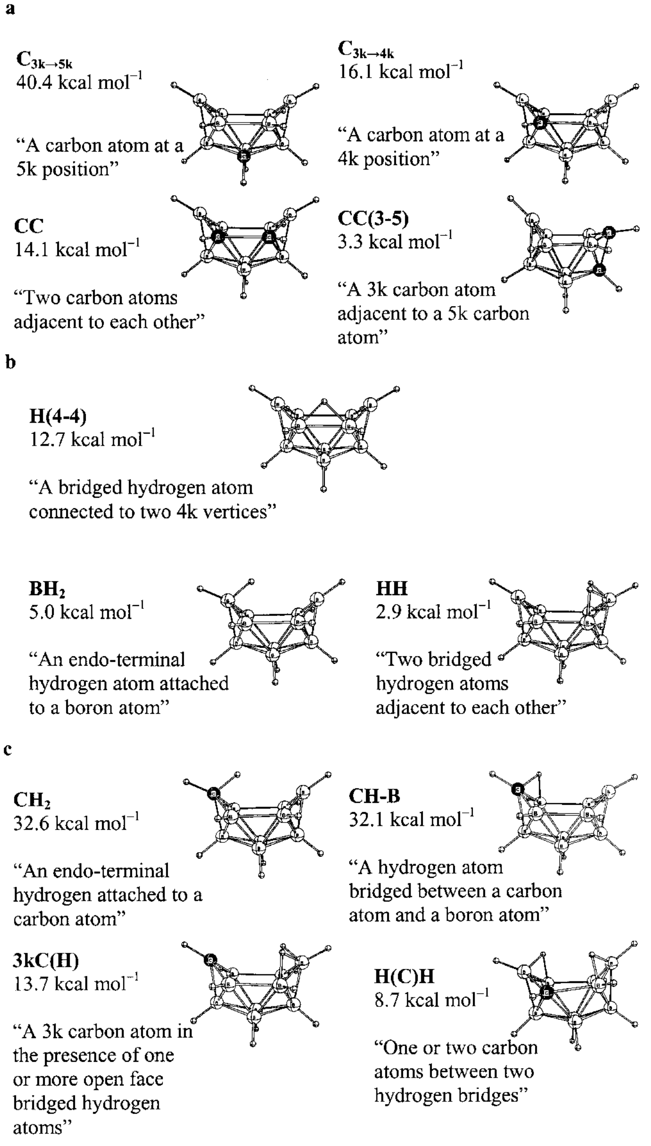

Figure 2. a) Carbon, b) hydrogen, and c) mixed structural features and their energy penalties.

A Comparison of Energy Penalties Between the 10-Vertex *nido* Cluster and the 6- and 11-Vertex *nido* Clusters

Some structural features in the 10-vertex *nido* cluster are also present in the 6- and/or 11-vertex *nido* clusters, i.e. HH, CC, BH_2, CH–B, and $C_{3k\to5k}$. All the features that were identified for all three cluster sizes are summarized in Table 1. Four comparable features are carbon structural features, one is a hydrogen structural feature, and two are mixed structural features. The remainder are entirely new and are described in the next section.

$C_{3k\to4k}$

Moving a carbon atom from a 3*k* vertex to a 4*k* vertex in the 10-vertex *nido* cluster requires 16.1 kcal mol^{-1}. This energy penalty is not observed in 6- or 11-vertex *nido* clusters because they lack 4*k* and 3*k* vertices, respectively.

$C_{3k\to5k}$

Moving a carbon atom from a 3*k* position to a 5*k* position involves an energy penalty of 40.4 kcal mol^{-1} in the 10-vertex *nido* cluster. The corresponding energy penalty in the 6-vertex *nido* cluster is 33 kcal mol^{-1}.

$C_{4k\to5k}$

This is not an independent structural feature of the 10-vertex *nido* cluster, but an energy penalty of 24.3 kcal mol^{-1} can be derived for it as the difference between $E_{\text{inc}}[C_{3k\to4k}]$ and $E_{\text{inc}}[C_{3k\to5k}]$. This value is quite close to the value of 28.0 kcal mol^{-1} for $C_{4k\to5k}$ in the 11-vertex *nido* cluster.[2]

CC

The CC energy penalty is essentially independent of the cluster size: values of 15, 14.1, and 16.0 kcal mol^{-1} apply for the 6-, 10-, and 11-vertex *nido* clusters, respectively.

HH

Two hydrogen bridges adjacent to each other, HH, have an energy penalty of 7 kcal mol^{-1} in the case of 6-vertex *nido*-boranes and -carboranes. This value is much larger (25.9 kcal mol^{-1}) in the case of 11-vertex *nido*-boranes and -carboranes. For the 10-vertex *nido* cluster, the energy penalty associated with HH is 2.9 kcal mol^{-1}. Hence, HH has very different energy penalties for the 6-, 10-, and 11-vertex *nido* clusters, although it should be kept in mind that the bridged hydrogen atoms have different connectivities in all these cases. In the case of 6-vertex *nido* clusters the bridged hydrogen atoms are connected to 3*k* peripheral vertices, whereas in the 11-vertex *nido* cluster the bridged hydrogen atoms are attached to all 4*k* peripheral vertices. In the case of a 10-vertex *nido* cluster, however, they are connected to a 3*k* vertex (6 or 9) on one side and to a 4*k* vertex on the other side.

CH–B

This has very similar energy penalties of 27, 32.1, and 33.1 kcal mol^{-1} in the 6-, 10-, and 11-vertex *nido* clusters, respectively.

CH_2

An *endo*-terminal hydrogen atom attached to a carbon atom in the 10-vertex *nido* cluster has an energy penalty of 32.6 kcal mol^{-1}, which is quite close to the CH_2 energy penalty of 30 kcal mol^{-1} and 33.2 kcal mol^{-1}for the 6-vertex and 11-vertex *nido* clusters, respectively. In the structure **JM**, there are two CH_2 moieties, each accompanied by one imaginary frequency.

In summary, carbon-related and mixed structural features are independent of cluster size.

New Structural Features for the 10-Vertex *nido* Cluster

There are four architectural features in the 10-vertex *nido*-boranes and -carboranes that are not present or not important in 6- and 11-vertex *nido*-boranes and -carboranes. These features are H(4–4), CC(3–5), 3*k*C(H), and H(C)H (see Figure 2). H(4–4) will be discussed later and H(C)H has already been discussed above. Here only CC(3–5) and 3*k*C(H) will be discussed.

CC(3–5)

When a 3*k* and a 5*k* carbon atom are adjacent to each other in the 10-vertex *nido* cluster, the energy penalty (3.3 kcal mol^{-1}) is only about one fourth of the CC value. This characteristic feature is accompanied by the distortion of the cluster structure in such a way that the 3*k* carbon atom lies almost in the plane of the 4*k* vertices [5,7,8,10, see Figure 2a, CC(3–5)]. This distortion counteracts the destabilization of the CC relationship and results in a diminished E_{inc}[CC(3–5)]. For the 6-vertex *nido* cluster a 3*k*–5*k* CC behaves the same way as a 3*k*–3*k* CC, but CC(3–3) is not possible in the 10-vertex cluster. Similarly, in the case of the 11-vertex *nido* cluster the energy penalty for a 4*k*–4*k* CC is the same as for 4*k*–5*k* CC or 5*k*–5*k* CC. In the 10-vertex *nido* cluster, CC(3–5) leads to significantly less destabilization as compared to more homogeneous CC relationships (3*k*–4*k*, 4*k*–4*k*, 4*k*–5*k*).

3kC(H)

A carbon atom at a 3*k* vertex in the presence of one or more open-face hydrogen bridges results in a thermodynamic stability reduction of 13.7 kcal mol^{-1}. This feature is not observed in $[C_2B_8H_{10}]^{2-}$, where there are no open-face hydrogen bridges, although it is present in 6,9-$C_2B_8H_{12}$ (Figure 3, **JS**). When there is an *endo*-terminal hydrogen atom at a 3*k* carbon atom (CH_2), or a bridged hydrogen atom between a carbon atom and a boron atom (CH–B), the 3*k*C(H) feature is not possible and no extra energy penalty is counted.

Hydrogen Placement Patterns

Hydrogen Bridges Occupy the Positions of Least Connectivity

In the 6- and 11-vertex clusters, there is only one kind of peripheral vertex each, and consequently all open-face edges are equally suited for hydrogen bridges. However, the open-face edges available for hydrogen bridges are not equivalent in the 10-vertex *nido* cluster due to different peripheral vertices. In all thermodynamically most stable isomers, the hydrogen bridges are located at 3*k*–4*k* edges. A hydrogen bridge between two 4*k* vertices, H(4–4), is 12.7 kcal mol^{-1} less stable [see Figure 2b, H(4–4)].

Hydrogen Placement Patterns are Primary to Carbon Placement Patterns

Williams' qualitative carbon placement rules[4,5] are quantitatively covered by $C_{3k\rightarrow4k}$, $C_{3k\rightarrow5k}$ and CC (see above). In the presence of extra hydrogen atoms, however, some more rules are needed. Figure 3 shows the 6,9- and 5,7-isomers of $C_2B_8H_{12}$[6,7] and their dianions.[8,9] A comparison of $[C_2B_8H_{10}]^{2-}$ and $C_2B_8H_{12}$ isomers demonstrates that carbon atoms occupy the least coordinated positions only when extra hydrogen atoms are absent. For example, *nido*-$[C_2B_8H_{10}]^{2-}$ (**HA**), without any *endo*-hydrogen atom, is the most stable $[C_2B_8H_{10}]^{2-}$ isomer as carbon atoms favor the positions of least connectivity. The doubly protonated *nido*-6,9-$C_2B_8H_{12}$ (**JS**), with bridging hydrogen atoms at positions 5/10 and 7/8, accumulates three structural features [H(4–4), 3kC(H), and H(C)H, each present twice], corresponding to a total energy penalty of 70.2 kcal mol^{-1}. This is 35.1 kcal mol^{-1} more than that of the most stable 5,7-$C_2B_8H_{12}$ (**JA**), where the carbon atoms are at positions of higher connectivity, i.e. $C_{3k\rightarrow4k}$ and HH are present. The computed energy difference is 44.5 kcal mol^{-1}.

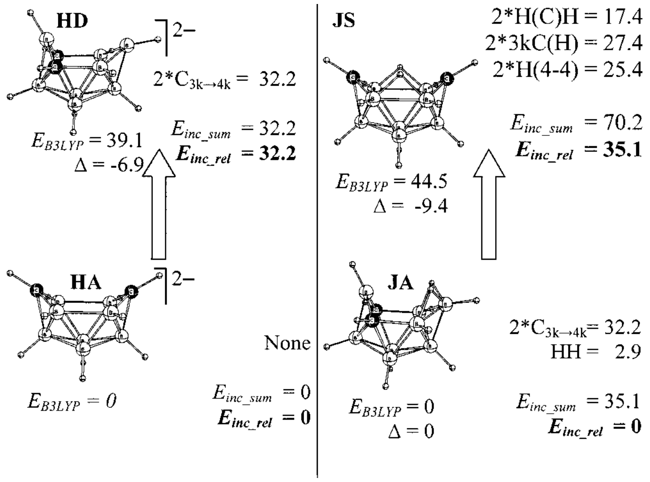

Figure 3. 6,9- and 5,7-isomers of $[C_2B_8H_{10}]^{2-}$ and $C_2B_8H_{12}$.

Comparisons of Relative Stabilities from Empirical Energy Penalties ($E_{\text{inc\_rel}}$) and from DFT-Calculated Values (E_{B3LYP}) for 10-Vertex *nido*-Boranes and -Carboranes

Initially, energy penalties for those structural features that were already found to be important for 6- and 11-vertex *nido*-boranes and -carboranes[1,2] were considered. 10-Vertex *nido*-boranes and -carboranes were found to have some features common with their 6- and 11-vertex counterparts, but some additional features are needed. The final set of structural features is shown in Figure 2 and listed in Tables 2–6 (see below). A total of eighty-one 10-vertex *nido*-borane and -carborane isomers from $[B_{10}H_{12}]^{2-}$ to $C_3B_7H_{11}$ were computed, ten of which are known experimentally. The sum of energy penalties for all structural features gives $E_{\text{inc\_sum}}$ for each structure, which relative to the most stable isomer (isomer with least $E_{\text{inc\_sum}}$) gives $E_{\text{inc\_rel}}$. Computed relative energies are listed as E_{B3LYP}. The difference between $E_{\text{inc\_rel}}$ and E_{B3LYP} (E_{diff}) is equal to, or larger than, 6 kcal mol^{-1} in only six cases. The largest deviation (Δ = –9.4 kcal mol^{-1}) is found for **JS** (6,9-$C_2B_8H_{12}$). Three $C_4B_6H_{10}$ isomers were computed but four carbon atoms in the 10-vertex *nido* cluster behave far less additively and cause large deviations (see Table 6 below). Tetracarboranes seem to have considerable hydrocarbon character. In the case of 6-vertex and 11-vertex *nido* clusters, the largest deviations are also observed for tetracarboranes. Our 10-vertex *nido*-(car)boranes study concentrates on mono- to tricarboranes.

nido-$[B_{10}H_{10+x}]^{(4-x)-}$ (*x* = 2–4) Isomers

Three structures have already been computed for *nido*-$[B_{10}H_{12}]^{2-}$ and the correct solution structure was reported to have μ-H: 5/6, 8/9 (**AA**, Figure 4).[10] Our increment system also predicts **AA** to be the most stable due to the absence of any structural feature (Table 2). Structure **AB** is slightly higher in energy than **AA** due to the structural feature HH. **AC**, with one imaginary frequency, has the structural feature H(4–4) twice due to two hydrogen atoms bridging two 4*k* vertices.

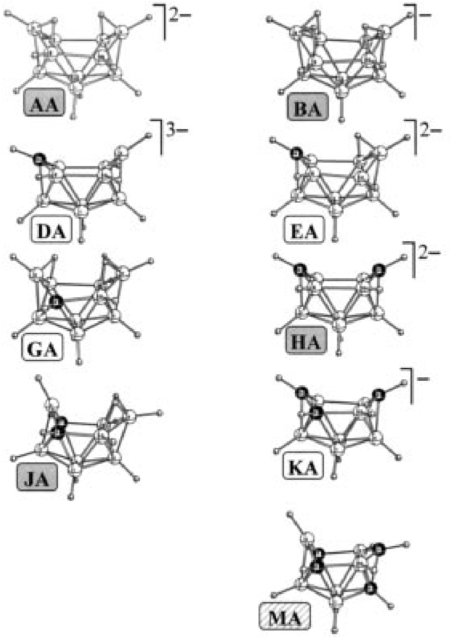

Figure 4. Most-stable isomers from *nido*-$[B_{10}H_{12}]^{2-}$ to -$C_4B_6H_{10}$. Known isomers are labeled with gray boxes. Those filled diagonally with grey lines are strong candidates for synthesis.

$B_{10}H_{14}$ (**CA**) can be easily deprotonated to give $[B_{10}H_{13}]^{-}$.[11] **BA**, (Figure 4) with bridging hydrogen atoms at the 5/6, 6/7, and 8/9 positions,[12] is the most stable $[B_{10}H_{13}]^{-}$ structure,[10] with only one structural feature, i.e. HH, as two hydrogen bridges at the 5/6 and 6/7 positions are adjacent to each other (Table 2). Hydrogen bridges at the 5/10, 6/7, and 8/9 positions (**BB**) involve one structural feature H(4–4). **BC** with one *endo*-H (structural feature BH_2) at position number 5 (a 4*k* vertex) is the transition state for a facile hydrogen rearrangement from the structure with bridging hydrogen atoms in the 5/6, 6/7, and 8/9 positions (**BA**) to the structure with bridging hydrogen atoms in the 6/7, 8/9, and 5/10 bridging positions (**BB**). **BD**, with BH_2 and HH, is the least favorable of the four isomers considered here. Two $B_{10}H_{14}$ structures were computed and the experimentally found structure[13] with four hydrogen atoms bridging to B5/6, B6/7, B8/9, and B9/10 positions (**CA**) was found to be computationally more stable than the structure with bridging hydrogen atoms at the 7/8 and 5/10 positions and an *endo*-H at 6,9 (**CB**, which corresponds to the prototypical 10-vertex *arachno* structure) by 38.1 kcal mol⁻¹. **CA** has the structural feature HH twice, but **CB** has the structural features 2 BH_2 + 2 H(4–4), with an $E_{\text{inc\_rel}}$ of 29.6 kcal mol⁻¹ with respect to **CA**. The difference between the computed and incremented relative energies (E_{diff}) is 8.5 kcal mol⁻¹.

nido-$[CB_9H_{10+x}]^{(3-x)-}$ (*x* = 0–3) Isomers

nido-6-$[CB_9H_{10}]^{3-}$ (**DA**, Figure 4) is the most stable $[CB_9H_{10}]^{3-}$ isomer, with the carbon atom at a 3*k* position (Table 3). *nido*-5-$[CB_9H_{10}]^{3-}$ (**DB**), with the $C_{3k\rightarrow 4k}$ structural feature [$E_{\text{inc}}(C_{3k\rightarrow 4k})$ = 16.1 kcal mol⁻¹], is thermodynamically 17.1 kcal mol⁻¹ less stable than **DA**. The carbon atom is at a 5*k* position (structural feature $C_{3k\rightarrow 5k}$) in *nido*-2-$[CB_9H_{10}]^{3-}$ (**DC**) and *nido*-1-$[CB_9H_{10}]^{3-}$ (**DD**), although **DC** is slightly more favorable. A “fine tuning increment” may be applied to differentiate between a 5*k* carbon atom at positions 1,3 (less favorable) and a 5*k* carbon atom at positions 2,4. A similar effect was also reported for the 11-vertex *nido* cluster where all vertices next to the apex (vertex number 1) are 5*k* but two vertices next to positions 2–6 are 4*k* and hence the apical position is slightly less favorable than positions 2–6.[2,3]

Table 2. Structural features and relative energies [kcal mol⁻¹] for $[B_{10}H_{12}]^{2-}$ and $[B_{10}H_{13}]^{-}$ isomers.

	Compound	Extra hydrogen atoms	Symmetry	H(4-4)	BH_2	HH	$E_{\text{inc\_sum}}$	$E_{\text{inc\_rel}}$	E_{B3LYP}	E_{diff}[a]
				12.7	5.0	2.9				
AA[b]	$B_{10}H_{12}{}^{2-}$	μ-H: 5/6, 8/9	C_2				0	0	0	0
AB	$B_{10}H_{12}{}^{2-}$	μ-H: 8/9, 9/10	C_s			1	2.9	2.9	3.4	–0.5
AC[c]	$B_{10}H_{12}{}^{2}$	μ-H: 5/10, 7/8	C_s	2			25.4	25.4	21.8	3.8
BA[a]	$B_{10}H_{13}{}^{1-}$	μ-H: 5/6, 6/7, 9/10	C_1			1	2.9	0	0	0
BB	$B_{10}H_{13}{}^{1-}$	μ-H: 5/10, 6/7, 8/9	C_1	1			12.7	12.7	3.9	7.8
BC[c]	$B_{10}H_{13}{}^{1-}$	μ-H: 6/7, 8/9 *endo*-H: 5	C_1		1		5.0	5.0	4.9	1.0
BD[c]	$B_{10}H_{13}{}^{1-}$	μ-H: 5/6, 6/7 *endo*-H: 9	C_s		1	1	7.9	7.9	13.4	–5.5
CA[b]	$B_{10}H_{14}$	μ-H: 5/6, 6/7, 8/9, 9/10	C_{2v}			2	5.8	0.0	0.0	0.0
CB	$B_{10}H_{14}$	μ-H: 7/8, 5/10, *endo*-H: 6,9	C_{2v}	2	2		35.4	29.6	38.1	–8.5

[a] E_{diff} is the difference between $E_{\text{inc\_rel}}$ and E_{B3LYP}. [b] Experimentally known structures. [c] **AC**, **BC**, and **BD** possess imaginary frequencies.

Table 3. Structural features and relative energies [kcal mol^{-1}] for $[CB_9H_{10+x}]^{3-x}$ (x = 0–3) isomers.

	Compound	Extra hydrogen atoms	Symmetry	H(4–4)	BH_2	HH	$C_{3k\rightarrow5k}$	$C_{3k\rightarrow4k}$	CH_2	CH–B	3kC(H)	H(C)H	E_{inc_sum}	E_{inc_rel}	E_{B3LYP}	E_{diff}[a]
				12.7	5.0	2.9	40.4	16.1	32.6	32.1	13.7	8.7				
DA	$6\text{-}CB_9H_{10}{}^{3-}$	–	C_s										0.0	0.0	0.0	0.0
DB	$5\text{-}CB_9H_{10}{}^{3-}$	–	C_1					1					16.1	16.1	17.1	–1.0
DC	$2\text{-}CB_9H_{10}{}^{3-}$	–	C_s				1						40.4	40.4	37.1	3.3
DD	$1\text{-}CB_9H_{10}{}^{3-}$	–	C_s				1						40.4	40.4	38.9	1.5
EA	$6\text{-}CB_9H_{11}{}^{2-}$	μ-H: 8/9	C_1								1		13.7	0	0	0
EB	$5\text{-}CB_9H_{11}{}^{2-}$	*endo*-H: 9	C_1		1			1					21.1	7.4	8.6	–1.2
EC	$6\text{-}CB_9H_{11}{}^{2-}$	*endo*-H: 6	C_s						1				32.6	18.9	13.3	5.6
ED	$1\text{-}CB_9H_{11}{}^{2-}$	μ-H: 7/8	C_s	1			1						53.1	39.4	48.1	–8.7
FA[b]	$6\text{-}CB_9H_{12}{}^{1-}$	μ-H: 8/9, 9/10	C_s			1					1		16.7	0	0	0
FB	$5\text{-}CB_9H_{12}{}^{1-}$	μ-H: 8/9, 9/10	C_1			1		1					19.1	2.4	6.6	–4.2
FC	$5\text{-}CB_9H_{12}{}^{1-}$	μ-H: 6/7, 9/10	C_1					1				1	24.8	8.2	12.7	–4.5
FD	$6\text{-}CB_9H_{12}{}^{1-}$	μ-H: 5/6, 8/9	C_1							1			32.1	15.5	15.6	–0.1
FE	$2\text{-}CB_9H_{12}{}^{1-}$	μ-H: 8/9, 9/10	C_s			1	1						43.4	26.7	30.5	–3.7
FF	$1\text{-}CB_9H_{12}{}^{1-}$	μ-H: 8/9, 9/10	C_1			1	1						43.4	26.7	30.7	–4.0
GA	$5\text{-}CB_9H_{13}$	μ-H: 6/7, 8/9, 9/10	C_1			1		1				1	27.8	0	0	0
GB[c]	$6\text{-}CB_9H_{13}$	μ-H: 8/9, 9/10; *endo*-H: 6	C_s			1			1				35.6	7.8	11.2	–3.4
GC	$2\text{-}CB_9H_{13}$	μ-H: 6/7, 8/9, 9/10	C_1			1	1						43.4	15.6	20.1	–4.5
GD	$1\text{-}CB_9H_{13}$	μ-H: 6/7, 8/9, 9/10	C_1			1	1						43.4	15.6	21.6	–6.0
GE	$1\text{-}CB_9H_{13}$	μ-H: 5/6, 7/8, 9/10	C_s	1				1				1	61.8	34.0	29.6	4.5

[a] E_{diff} is the difference between E_{inc_rel} and E_{B3LYP}. [b] **FA** is an experimentally known structure. [c] **GB** has one imaginary frequency.

The most stable *nido*-6-$[CB_9H_{11}]^{2-}$ structure (**EA**, Figure 4) has one structural feature, i.e. 3kC(H), as a 3k carbon atom and a bridged hydrogen atom are present. *nido*-5-$[CB_9H_{11}]^{2-}$ (**EB**) has an *endo* hydrogen atom (structural feature BH_2) in addition to $C_{3k\rightarrow4k}$. **EC** differs with respect to the most stable isomer **EA** only in the positions of the hydrogen atom on the open face (the *endo*-terminal hydrogen atom on the carbon atom results in the high-energy structural feature CH_2 in **EC**). *nido*-1-$[CB_9H_{11}]^{2-}$ (**ED**) is highly unstable due to the presence of a carbon atom at a 5k position ($C_{3k\rightarrow5k}$).

Experimentally known[14] *nido*-6-$[CB_9H_{12}]^{-}$ (**FA**, Figure 4) has two structural features, HH and 3kC(H), each once. Both **FB** and **FC** have the carbon atom at vertex number 5 ($C_{3k\rightarrow4k}$), but different hydrogen positions result in one HH (two adjacent hydrogen bridges) in the former and H(C)H (a carbon atom between two hydrogen bridges) in the latter. The energy penalty for H(C)H is larger than that for HH, and therefore **FC** is suggested to be more favorable than **FB**, both computationally as well as by the increment system. The basic skeleton of *nido*-6-$[CB_9H_{12}]^{-}$ (**FD**) is identical to that of the most stable **FA** except that hydrogen atoms are bridging positions 5/6 and 8/9 in the latter but 8/9 and 9/10 in the former. The special hydrogen position in **FD** (a hydrogen atom is bridging a carbon atom and a boron atom) gives rise to the structural feature CH–B, with E_{inc}(CH–B) = 32.1 kcal mol^{-1}, and is responsible for the high relative energy of the cluster even though the carbon atom is situated at a least connected vertex. Each of the *nido*-2-$[CB_9H_{12}]^{-}$ (**FE**) and *nido*-1-$[CB_9H_{12}]^{-}$ (**FF**) clusters possess the structural features HH and $C_{3k\rightarrow5k}$, but the carbon atom at position 1 in **FF** is slightly more disfavoring.

The experimentally unknown *nido*-5-CB_9H_{13} (**GA**, Figure 4) is the most favorable CB_9H_{13} structure. The structural features, corresponding energy penalties, and relative stabilities of the five computed CB_9H_{13} isomers are listed in Table 3.

The relative stabilities of the 6- and 5-isomers of *nido*-$[CB_9H_{10+x}]^{3-x}$ (x = 0–3) are as follows: *nido*-6-$[CB_9H_{10}]^{3-}$ (**DA**) is 17.1 kcal mol^{-1} more stable than *nido*-5-$[CB_9H_{10}]^{3-}$ (**DB**), and *nido*-6-$[CB_9H_{11}]^{2-}$ (**EA**) and *nido*-6-$[CB_9H_{12}]^{-}$ (**FA**) are 8.6 and 6.6 kcal mol^{-1} more stable than their 5-isomers (**EB** and **FB**, respectively). However, in the case of the neutral clusters, 6-CB_9H_{13} (**GB**) is 11.2 kcal mol^{-1} less stable than *nido*-5-CB_9H_{13} (**GA**). An increased hydrogen content on the open face results in highly connected carbon atoms in the most stable isomer, as is observed in the case of 11-vertex *nido*-$CB_{10}H_{14}$.[2] This can be well explained in terms of the structural features. E_{inc_sum} for the different structural features of **DB**, **EB**, and **FB** is less than that of **DA**, **EA**, and **FA**; however, E_{inc_sum} favors 5-CB_9H_{13} (**GA**; E_{inc_sum} = 27.8 kcal mol^{-1}) rather than 6-CB_9H_{13} (**GB**; E_{inc_sum} = 35.6 kcal mol^{-1}) mainly due to the high-energy structural feature (CH_2) in the latter. No *nido*-CB_9H_{13} isomer is experimentally known. However, the computed (HF/6-31G*) geometry for *nido*-6-CB_9H_{13} (**GB**) has been reported.[15]

nido-$[C_2B_8H_{10+x}]^{(2-x)-}$ (x = 0–2)

Two structures, i.e. the most stable *nido*-6,9-$[C_2B_8H_{10}]^{2-}$ (**HA**, Figure 4),[8] and *nido*-5,7-$[C_2B_8H_{10}]^{2-}$ (**HD**),[9] are experimentally known. Three structural features, i.e. $C_{3k\rightarrow4k}$, $C_{3k\rightarrow5k}$, and CC reproduce the relative stability of any possible $C_2B_8H_{10}{}^{2-}$ isomer (see Table 4) as there are no hydrogen atoms. *nido*-6,9-$[C_2B_8H_{10}]^{2-}$ (**HA**) has no structural features as the carbon atoms are at the nonadjacent least-connected vertices. Addition of one bridging hydrogen atom to **HA** makes the situation highly unfavorable in *nido*-6,9-$[C_2B_8H_{11}]^{-}$ (**IC**) due to one H(4–4) and two 3kC(H) structural features. One carbon atom is located at a 4k vertex in the most stable *nido*-5,9-$[C_2B_8H_{11}]^{-}$ (**IA**, Figure 4), for which the sum of the energy penalties is less than that of **IC**. Experimentally known *nido*-5,6-$[C_2B_8H_{11}]^{-}$ (**ID**)[16] is higher in energy than its three unknown isomers *nido*-5,9-$[C_2B_8H_{11}]^{-}$ (**IA**), *nido*-5,7-$[C_2B_8H_{11}]^{-}$ (**IB**), and *nido*-6,9-$[C_2B_8H_{11}]^{-}$ (**IC**). *nido*-2,6-$[C_2B_8H_{11}]^{-}$ (**IE**), which contains the structural feature CC(3–5) as well as $C_{3k\rightarrow5k}$ and 3kC(H), is the highest-energy structure.

nido-5,7-$C_2B_8H_{12}$ (**JA**, Figures 3 and 4)[6] is the most stable neutral dicarba isomer (Table 5). *nido*-5,6-$C_2B_8H_{12}$

Table 4. Structural features and relative energies [kcal mol^{-1}] for $[C_2B_8H_{10+x}]^{2-x}$ ($x = 0, 1$) isomers.

	Compound	Extra hydrogen atoms	Symmetry	H(4–4)	BH_2	HH	$C_{3k\rightarrow 5k}$	$C_{3k\rightarrow 4k}$	CC	CC(3–5)	3*k*C(H)	E_{inc_sum}	E_{inc_rel}	E_{B3LYP}	E_{diff}[a]
				12.7	5.0	2.9	40.4	16.1	14.1	3.3	13.7				
HA[b]	6,9-$C_2B_8H_{10}{}^{2-}$	–	C_{2v}									0	0	0	0
HB[c]	5,9-$C_2B_8H_{10}{}^{2-}$	–	C_1					1				16.1	16.1	14.4	1.7
HC[c]	5,8-$C_2B_8H_{10}{}^{2-}$	–	C_2					2				32.2	32.2	35.0	–2.8
HD[b]	5,7-$C_2B_8H_{10}{}^{2-}$	–	C_s					2				32.2	32.2	39.1	–6.9
HE	2,6-$C_2B_8H_{10}{}^{2-}$	–	C_s				1			1		43.8	43.8	43.0	0.8
HF	5,10-$C_2B_8H_{10}{}^{2-}$	–	C_s					2	1			43.3	43.3	48.0	–4.7
HG	1,5-$C_2B_8H_{10}{}^{2-}$	–	C_1				1	1	1			70.7	70.7	71.0	–0.3
HH	2,4-$C_2B_8H_{10}{}^{2-}$	–	C_{2v}				2					80.9	80.9	75.0	5.9
HI	1,3-$C_2B_8H_{10}{}^{2-}$	–	C_{2v}				1		1			95.0	95.0	92.0	3.0
IA[c]	5,9-$C_2B_8H_{11}{}^{1-}$	μ-H: 6/7	C_1					1			1	29.8	0	0	0
IB[c]	5,7-$C_2B_8H_{11}{}^{1-}$	*endo*-H: 9	C_s		1			2				37.2	7.4	9.4	–2.0
IC[c]	6,9-$C_2B_8H_{11}{}^{1-}$	μ-H: 7/8,	C_s	1							2	40.1	10.3	9.4	0.8
ID[b]	5,6-$C_2B_8H_{11}{}^{1-}$	μ-H: 8/9	C_1					1	1		1	43.9	14.1	16.4	–2.3
IE	2,6-$C_2B_8H_{11}{}^{1-}$	μ-H: 8/9	C_1				1			1	1	57.4	27.5	29.9	–2.4

[a] E_{diff} is the difference between E_{inc_rel} and E_{B3LYP}. [b] Experimentally known isomers. [c] Strong candidates for synthesis.

Table 5. Structural features and relative energies [kcal mol^{-1}] for $C_2B_8H_{12}$ isomers.

	Compound	Extra hydrogen atoms	Symmetry	H(4–4)	BH_2	HH	$C_{3k\rightarrow 5k}$	$C_{3k\rightarrow 4k}$	CC	CC(3–5)	CH_2	CH–B	3kC(H)	H(C)H	E_{inc_sum}	E_{inc_rel}	E_{B3LYP}	E_{diff}[a]
				12.7	5.0	2.9	40.4	16.1	14.1	3.3	32.6	32.1	13.7	8.7				
JA[b]	5,7-$C_2B_8H_{12}$	μ-H: 8/9, 9/10	C_s			1		2							35.1	0	0	0
JB[c]	5,9-$C_2B_8H_{12}$	μ-H: 6/7, 9/10	C_1					1				1			48.2	13.1	11.3	1.8
JC[c]	5,8-$C_2B_8H_{12}$	μ-H: 6/7, 9/10	C_1					2						1	49.6	14.5	11.6	3.0
JD[b]	5,6-$C_2B_8H_{12}$	μ-H: 8,9, 9/10	C_1			1		1	1				1		46.8	11.7	15.1	–3.4
JE	1,6-$C_2B_8H_{12}$	μ-H: 8/9, 9/10	C_1			1	1						1		57.0	21.9	20.7	1.2
JF	5,10-$C_2B_8H_{12}$	μ-H: 6/7, 8/9	C_s					2	1					1	55.1	20.0	22.3	–2.4
JG	4,6-$C_2B_8H_{12}$	μ-H: 8/9, 9/10	C_s			1	1						1		59.4	21.9	24.2	–2.3
JH	1,7-$C_2B_8H_{12}$	μ-H: 8/9, 9/10	C_1			1	1	1							59.4	24.3	24.3	0
JI	2,10-$C_2B_8H_{12}$	μ-H: 5/6, 6/7	C_1			1	1	1							59.4	24.3	25.7	–1.4
JJ	2,6-$C_2B_8H_{12}$	μ-H: 8/9, 9/10	C_s			1	1			1			1		60.3	25.2	26.0	–0.8
JK	6,9-$C_2B_8H_{12}$	μ-H: 6/7, 8/9	C_s									2			64.2	29.1	32.1	–0.7
JL	1,7-$C_2B_8H_{12}$	μ-H: 5/6, 8/9	C_1				1	1						1	65.2	30.1	33.8	–3.7
JM[d]	6,9-$C_2B_8H_{12}$	*endo*-H: 6,9	C_{2v}								2				65.2	30.1	35.3	–5.2
JN	1,7-$C_2B_8H_{12}$	μ-H: 5/10; *endo*-H:9	C_1	1	1		1	1							74.1	39.0	36.4	2.7
JO	2,7-$C_2B_8H_{12}$	μ-H: 5/6, 9/10	C_1				1	1	1						70.6	35.5	37.9	–2.4
JP	2,7-$C_2B_8H_{12}$	μ-H: 8/9, 9/10	C_1			1	1	1	1						73.5	38.4	38.4	0
JQ	1,5-$C_2B_8H_{12}$	μ-H: 6/7, 8/9	C_1				1	1	1						70.6	35.5	41.0	–5.5
JR	6,8-$C_2B_8H_{12}$	μ-H: 5/6; *endo*-H: 8	C_1					1			1	1			80.8	45.7	41.7	4.0
JS	6,9-$C_2B_8H_{12}$	μ-H: 5/10, 7/8	C_{2v}	2									2	2	70.2	35.1	44.5	–9.4
JT	3,7-$C_2B_8H_{12}$	μ-H: 5/6, 8/9	C_1				1	1	1					1	79.4	44.3	48.7	–4.4
JU	2,4-$C_2B_8H_{12}$	μ-H: 8/9, 9/10	C_s			1	2								83.7	48.6	52.1	–3.5
JV	1,3-$C_2B_8H_{12}$	μ-H: 8/9, 9/10	C_s			1	2		1						97.8	62.7	63.5	–0.8
JW	1,2-$C_2B_8H_{12}$	μ-H: 8/9, 9/10	C_1			1	2		1						97.8	62.7	64.4	–1.7
JX	1,2-$C_2B_8H_{12}$	μ-H: 5/6, 8/9	C_1				2		1						94.9	59.8	64.8	–5.0
JY	1,2-$C_2B_8H_{12}$	μ-H: 5/6, 6/7	C_1			1	2		1						97.8	62.7	65.2	–2.5
JZ	1,2-$C_2B_8H_{12}$	μ-H: 5/10, 6/7	C_1				2		1					1	1.03.7	68.8	65.8	2.7
JAA	1,3-$C_2B_8H_{12}$	μ-H: 6/7, 8/9	C_s				2		1					1	1.03.7	68.8	66.0	2.6
JAB	1,3-$C_2B_8H_{12}$	μ-H: 5/6, 8/9	C_2				2		1					1	103.7	68.8	66.5	2.1
JAC	1,2-$C_2B_8H_{12}$	μ-H: 5/10; *endo*-H: 6	C_1	1	1		2		1						112.6	77.5	72.1	5.4
JAD	1,2-$C_2B_8H_{12}$	μ-H: 5/6, 9/10	C_1				2		1					1	103.7	68.6	73.5	–5.0
JAE	1,2-$C_2B_8H_{12}$	μ-H: 5/10; *endo*-H: 9	C_1	1	1		2		1						112.6	77.5	74.3	3.1
JAF	1,3-$C_2B_8H_{12}$	μ-H: 7/8, 5/10	C_{2v}	2			2		1						120.3	85.2	85.5	–0.3

[a] E_{diff} is the difference between E_{inc_rel} and E_{B3LYP}. [b] Experimentally known isomer. [c] Strong candidate for synthesis. [d] **JM** has two imaginary frequencies.

(**JD**) and *nido*-5,7-$C_2B_8H_{12}$ (**JA**) represented the first case of skeletal isomers in *nido*-carboranes.[7] A large number of $C_2B_8H_{12}$ isomers (Table 5) was computed in order to obtain a reliable structural increment system for 10-vertex *nido*-carboranes. Calculated (HF/6-31G*) geometries for *nido*-6,9-$C_2B_8H_{12}$ (**JM**) and *nido*-6,9-$C_2B_8H_{12}$ (**JS**) have been reported before.[15]

nido-$[C_3B_7H_{10}]^-$ and -$C_3B_7H_{11}$

Three $[C_3B_7H_{10}]^-$ isomers have been computed, of which 5,6,9-$[C_3B_7H_{10}]^-$ (**KA**, Figure 4) is the most stable structure. Two *nido*-$C_3B_7H_{11}$ isomers are known: *nido*-5,6,9-$C_3B_7H_{11}$ (**LA**, Figure 4)[17] and *nido*-5,6,10-$C_3B_7H_{11}$ (**LD**), with a bridging hydrogen atom at the 7/8 position.[18] The increment system quite successfully reproduces the relative stability order of *nido*-$[C_3B_7H_{10}]^-$ and -$C_3B_7H_{11}$ structures (Table 6).

nido-$C_4B_6H_{10}$

The only known $C_4B_6H_{10}$ isomer is 5,6,8,9-$C_4B_6H_{10}$ (**MB**) reported by Stibr et al.,[19] but the 4,5,7,9-isomer (**MA**, Figure 4) is computed to be slightly preferred energetically (by 2.5 kcal mol^{-1}). For tetracarbaboranes from **MA** to **MG** (Table 6), deviations between the E_{B3LYP} and E_{inc_rel} are large when only the increments discussed above are applied. In the case of $C_4B_6H_{10}$, the four carbon atoms in a cluster result in a change of the behavior of carboranes, due to considerable hydrocarbon character. Hence, the additivity required by the increment system to be useful is not followed strictly and deviations of between 10.3 and

Table 6. Structural features and relative energies [kcal mol^{-1}] for 10-vertex *nido*-tri- and -tetracarboranes.

	Compound	Extra hydrogen atoms	Symmetry	$C_{3k\rightarrow 5k}$	$C_{3k\rightarrow 4k}$	CC	CC(3–5)	CH–B	3kC(H)	$(CC)_2$	E_{inc_sum}	E_{inc_rel}	E_{B3LYP}	E_{diff}[a]
				40.4	16.1	14.1	3.3	32.1	13.7	18.1				
KA	5,6,9-$C_3B_7H_{10}{}^{1-}$	–	C_1		1	1					30.2	0.0	0.0	0.0
KB	1,6,9-$C_3B_7H_{10}{}^{1-}$	–	C_s	1							40.4	10.2	7.6	2.4
KC	6,7,8-$C_3B_7H_{10}{}^{1-}$	–	C_1		2	2					60.4	30.2	24.0	6.2
LA[b]	5,6,8-$C_3B_7H_{11}$	μ-H: 9/10	C_1		2	1			1		60.0	0	0	0
LB[b]	5,6,9-$C_3B_7H_{11}$	μ-H: 6/7	C_1		1	1		1			62.3	2.3	3.4	–1.1
LC[c]	5,7,8-$C_3B_7H_{11}$	μ-H: 9/10	C_1		3	1					62.4	2.4	5.3	–2.9
LD[b]	5,6,10-$C_3B_7H_{11}$	μ-H: 8/9	C_1		2	2			1		74.1	14.1	9.0	5.2
MA[c]	4,5,7,9-$C_4B_6H_{10}$	–	C_1	1	2		1				76.0	0.0	0	0.0
MB[b]	5,6,8,9-$C_4B_6H_{10}$	–	C_2		2	2				1	78.5	2.5	2.5	0.0
MC	5,6,7,9-$C_4B_6H_{10}$	–	C_s		2	2				1	78.5	2.5	9.5	–7.0
MD	1,6,7,9-$C_4B_6H_{10}$	–	C_1	1	1	1					70.7	–5.3	11.1	–16.4
ME	1,5,7,9-$C_4B_6H_{10}$	–	C_1	1	2	1					86.8	10.8	11.8	–1.0
MF	5,7,8,10-$C_4B_6H_{10}$	–	C_{2v}		4	2				1	110.7	34.7	26.9	7.8
MG	2,4,6,9-$C_4B_6H_{10}$		C_{2v}	2			2			1	105.7	29.7	30.5	–0.8

[a] E_{diff} is the difference between E_{inc_rel} and E_{B3LYP}. [b] Experimentally known isomer. [c] Strong candidate for synthesis.

25.1 kcal mol^{-1} are observed. However, applying an extra increment [$(CC)_2$ = 18.1 kcal mol^{-1}] for the adjacent carbon atoms in the cluster twice lowers the energy differences considerably (Table 6), and only **MD** remains with a large deviation. Larger deviations of tetracarbaboranes are also observed in 6- and 11-vertex *nido* clusters.

Conclusions

An increment system has been established for 10-vertex *nido*-boranes and -carboranes. Eleven architectural features have been identified (eight of major importance, with E_{inc} > 5 kcal mol^{-1}, and three of minor importance). The corresponding energy penalties have allowed us to accurately estimate the relative stabilities of 81, and probably more, 10-vertex *nido* isomers from $[B_{10}H_{12}]^{2-}$ to $C_3B_7H_{11}$. Applying our increment system, ten carboranes have been identified that are not yet known experimentally but are thermodynamically more stable than known isomers and hence should be synthesizable.

The relative energies of 10-vertex *nido*-carboranes can be accurately predicted from $[B_{10}H_{12}]^{2-}$ to $C_3B_7H_{11}$ using the increment approach (Figure 5). In all the above examples, there are six cases where the difference between the estimated relative energy based on increments (E_{inc_rel}) and computed relative energy (E_{B3LYP}) is equal to, or more than, 6 kcal mol^{-1}. The difference between the E_{inc_rel} and E_{B3LYP} is less than 2 kcal mol^{-1} in 31 cases. The largest deviation, namely 9.4 kcal mol^{-1}, is found for 6,9-$C_2B_8H_{12}$ (**JS**). The stability order is mostly the same according to the B3LYP-computed results and to the increment approach. However, it is slightly different in many $C_2B_8H_{12}$ cases where the energetic separations of the many isomers considered is very small (see Table 5). The energy penalties for three features – CC, CH–B, and CH_2 – are very similar to those derived for the 6- and 11-vertex *nido*-(car)boranes. A fourth feature, $C_{4k\rightarrow 5k}$, also has an energy penalty quite similar to the 11-vertex *nido*-(car)borane value. This increment system is not limited to the representative 81 isomers it was derived from, but can be applied to many 10-vertex *nido*-carborane structures. A similar kind of increment system might be derivable for 10-vertex *nido*-heterocarboranes.

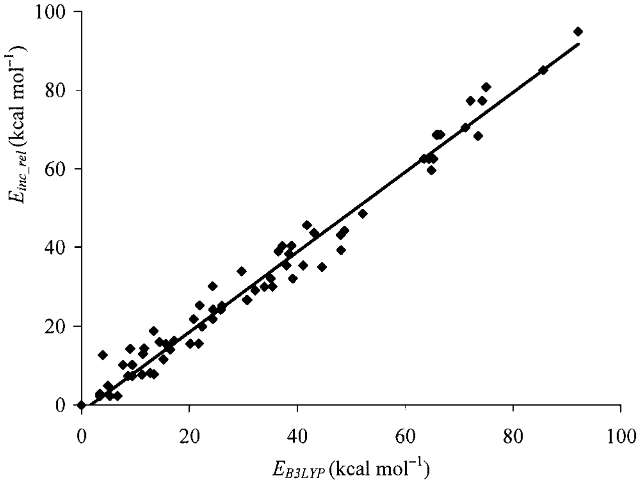

Figure 5. Structural increments accurately reproduce the relative stabilities of 10-vertex *nido*-(car)boranes computed by DFT methods.

Computational Details

Density functional theory was employed for successive optimization of all geometries at the B3LYP/3-21G and B3LYP/6-31G(d) levels, respectively, using the Gaussian 98 program.[20] Symmetry restrictions for different geometries, where applied, are given in Tables 2–6. All the structures, except five (**AC**, **BC**, **BD**, **GB** and **JM**, Tables 2, 3, and 5), presented in this paper are local minima at the B3LYP/6-31G(d) level as determined by frequency calculations. Single-point energies computed at the B3LYP/6-311+G(d,p) level, together with zero-point corrections at the B3LYP/6-31G(d) level, were used to derive relative energies for all the isomers. These computed relative energies are to be reproduced by a structural increment system. Certain geometrical features were identified and assigned reasonable preliminary energy penalties by comparison with suitable isomeric clusters. The values were refined through a statistical fitting procedure in order to obtain the final increment system. The Cartesian coordinates of structures fully optimized at the RB3LYP/6-31G(d) level and corresponding absolute energies from RB3LYP/6-311+G(d,p) energy computations are provided as Supporting Information.

Acknowledgments

Financial support by the Deutsche Forschungsgemeinschaft (DFG) is gratefully acknowledged.

---

[1] M. Hofmann, M. A. Fox, R. Greatrex, P. v. R. Schleyer, R. E. Williams, *Inorg. Chem.* **2001**, *40*, 1790–1801.

[2] F. A. Kiani, M. Hofmann, *Inorg. Chem.* **2004**, *43*, 8561–8571.

[3] F. A. Kiani, M. Hofmann, *Inorg. Chem.*, submitted.

[4] R. E. Williams, *J. Am. Chem. Soc.* **1965**, *87*, 3513–3515.

[5] R. E. Williams, in *Progress in Boron Chemistry* (Eds.: R. J. Brotherton, H. Steinberg), Pergamon Press, England, **1970**, vol. 2, chapter 2, p. 57.

[6] P. M. Garrett, G. S. Ditta, M. F. Hawthorne, *J. Am. Chem. Soc.* **1971**, *93*, 1265–1266.

[7] R. R. Rietz, R. Schaeffer, *J. Am. Chem. Soc.* **1973**, *95*, 6254–6262.

[8] B. Štíbr, J. Plešek, S. Heřmánek, *Collect. Czech. Chem. Commun.* **1973**, *38*, 338–342.

[9] B. Štíbr, Z. Janousek, K. Base, S. Heřmánek, J. Plešek, I. A. Zakharova, *Collect. Czech. Chem. Commun.* **1984**, *49*, 1891–1894.

[10] M. Hofmann, P. v. R. Schleyer, *Inorg. Chem.* **1998**, *37*, 5557–5565.

[11] G. A. Guter, G. W. Schaeffer, *J. Am. Chem. Soc.* **1956**, *78*, 3456.

[12] A. J. Wynd, A. J. Welch, *Acta Crystallogr., Sect. C* **1989**, *45*, 615–617.

[13] J. S. Kasper, C. M. Lucht, D. Harker, *Acta Crystallogr.* **1950**, *3*, 436–455.

[14] K. Base, B. Štíbr, J. Dolansky, J. Duben, *Collect. Czech. Chem. Commun.* **1981**, *46*, 2345–2353.

[15] M. L. McKee, *Inorg. Chem.* **1994**, *33*, 6213–6218.

[16] J. Zbyněk, P. Kaszynski, J. D. Kennedy, B. Štíbr, *Collect. Czech. Chem. Commun.* **1999**, *64*, 986–992.

[17] S. O. Kang, G. T. Furst, L. G. Sneddon, *Inorg. Chem.* **1989**, *28*, 2339–2347.

[18] A. E. Wille, L. G. Sneddon, *Collect. Czech. Chem. Commun.* **1997**, *62*, 1214–1228.

[19] B. Štíbr, T. Jelínek, E. Drdakova, S. Heřmánek, J. Plešek, *Polyhedron* **1988**, *7*, 669–670.

[20] M. J. Frisch, G. W. Trucks, H. B. Schlegel, G. E. Scuseria, M. A. Robb, J. R. Cheeseman, V. G. Zakrzewski, J. A. Montgomery Jr., R. E. Stratmann, J. C. Burant, S. Dapprich, J. M. Millam, A. D. Daniels, K. N. Kudin, M. C. Strain, O. Farkas, J. Tomasi, V. Barone, M. Cossi, R. Cammi, B. Mennucci, C. Pomelli, C. Adamo, S. Clifford, J. Ochterski, G. A. Petersson, P. Y. Ayala, Q. Cui, K. Morokuma, D. K. Malick, A. D. Rabuck, K. Raghavachari, J. B. Foresman, J. Cioslowski, B. J. V. Ortiz, B. Stefanov, G. Liu, A. Liashenko, P. Piskorz, I. Komaromi, R. Gomperts, R. L. Martin, D. J. Fox, T. Keith, M. A. Al-Laham, C. Y. Peng, A. Nanayakkara, C. Gonzalez, M. Challacombe, P. M. W. Gill, B. Johnson, W. Chen, M. W. Wong, J. L. Andres, C. Gonzalez, M. Head-Gordon, E. S. Replogle, J. A. Pople, *Gaussian 98*, Revision A.6, Gaussian, Inc., Pittsburgh PA, **1998**..

Received: November 26, 2004